The Synthesis, Structure, and FTIR Spectroelectrochemistry of W(CO)$_5$ Complexes of 4-Oxo-4-(2,5-dimethylazaferrocen-1′-yl)butanoic and 5-Oxo-5-(2,5-dimethylazaferrocen-1′-yl)pentanoic Acids

Konrad Kowalski,*[a] Rainer F. Winter,[b] Anna Makal,[c] Aleksandra Pazio,[c] and Krzysztof Woźniak[c]

With the aim of developing new IR-detectable metal–carbonyl tracers for the amino function, we have synthesized W(CO)$_5$ complexes of 4-oxo-4-(2,5-dimethylazaferrocen-1′-yl)butanoic acid (2) and 5-oxo-5-(2,5-dimethylazaferrocen-1′-yl)pentanoic acid (3) by AlCl$_3$-catalyzed Friedel–Crafts reaction of W(CO)$_5$–2,5-dimethylazaferrocene (1) with succinic or glutaric anhydride. Complexes 2 and 3 are thermally stable and display sharp, intense absorption bands of tungsten-coordinated CO ligands at ca. 1923 cm^{-1}. In the crystalline state, molecules of 2 and 3 are stabilized by a network of intra- and intermolecular hydrogen bonds, as shown by single-crystal X-ray structure analysis. Complex 2 was transformed into the corresponding N-succinimidyl ester 4. Its utility toward labeling of amino acids was tested in its reaction with glycine methyl ester. Corresponding glycine amide

5 was obtained in 82 % yield and is an air/thermally stable bioconjugate exhibiting intense sharp absorption bands of the W–CO reporting group at ca. 1923 cm^{-1}. Cyclic voltammetry of 1, 2, 3, and acetyl derivative 6 shows the presence of two redox events in each case. The first redox couple is ascribed as an azaferrocene-centered oxidation–reduction, whereas the second, irreversible process at higher potential originates from a W(CO)$_5$-centered oxidation. FTIR spectroelectrochemistry allowed us to monitor the spectroscopic changes accompanying the 1/1$^{·+}$, 2/2$^{·+}$, and 6/6$^{·+}$ redox transformations. Significant W–CO absorption band shifts were recorded in the course of these experiments.

Introduction

The application of metal–carbonyl derivatives (conjugates) in biology has recently attracted much interest. Metal–carbonyl components present in such molecules display sharp, intense absorption bands of metal-bound CO ligands in the 1850–2150 cm^{-1} region. This region is virtually free from absorption bands of biomolecules and biological matrices. Metal–carbonyl bioconjugates of steroids, herbicides, biotin, drugs, amino acids, proteins, and natural products have been reported, and their IR absorbances were used to quantify their concentrations in biological media.[1]

In the emerging field of organometallic anticancer agents, metal–carbonyl derivatives are also becoming increasingly important. It has been demonstrated, for exam-

ple, that tricarbonyliron complexes of nucleosides exhibit significant apoptosis-inducing properties,[2] whereas hexacarbonyldicobalt deoxyuridines display good antiproliferative activities toward human breast cancer cell lines.[3] An acetylenehexacarbonyldicobalt complex of o-acetylsalicylic acid has been recognized as an effective cyclooxygenase (COX) enzymes inhibitor,[4] and selected indocarbazole carbonyl ruthenium complexes were recognized as effective glycogen synthase kinase 3 inhibitors.[5] Hexacarbonyldicobalt derivatives of the neuropeptide leucine–enkephalin have also been described and represent the first organometallic peptide bioconjugates to exhibit significant toxicity against two different tumor cell lines.[6a] Recently, the synthesis and characterization of several new hexacarbonyldicobalt bioconjugates of amino acids, peptides, and peptide nucleic acids have been reported.[6b] Metal–carbonyls and their derivatives can be also utilized as CO-releasing molecules (CORMs).[7] Moreover, attachment of metal–carbonyls to cell penetrating peptide vectors[8] is a promising direction of research combining biological selectivity of specific peptides with the cytotoxic properties of their IR detectable organometallic "cargo". Another hot topic of bioorganometallic chemistry where metal–carbonyls have a role to play is the synthesis of complexes that model the hydrogenase active site.[1,9]

[a] Department of Organic Chemistry, Faculty of Chemistry, University of Łódź,
Narutowicza 68, 90-136 Łódź, Poland
E-mail: kondorl5@wp.pl
[b] Institut für Anorganische Chemie der Universität Regensburg,
Universitätsstraße 31, 93040 Regensburg, Germany
[c] Chemistry Department, Warsaw University,
Pasteura 1, 02-093 Warszawa, Poland
▣ Supporting information for this article is available on the WWW under http://dx.doi.org/10.1002/ejic.200900347.

Ferrocene and its derivatives can nowadays be termed as classical organometallics of biological interest. This is reflected by the tremendous number of papers, reviews, and books dealing with different applications of the ferrocenyl moiety in biological sciences.[1,10] Leading examples of biologically active ferrocene derivatives are anti-breast cancer active Ferrocifens and Hydroxyferrocifens.[11] Their antiproliferative effect arises from a combination of an antihormonal effect induced by the organic tamoxifen skeleton and a cytotoxic effect of the ferrocene moiety. Far less attention, however, has been dedicated to biological applications of heteroferrocenes.[12] In our opinion, heteroferrocenes offer a unique set of properties that possibly increase their biological spectrum of applications over those available with their simpler ferrocene counterparts. The presence of a nitrogen or phosphorus donor atom within the aza- and phosphaferrocene framework allows rich coordination chemistry of these complexes.[13] When the heterometallocene moiety is coordinated to the metal–carbonyl fragment such a system is capable of being detected by both electrochemical and IR spectroscopic methods, whereas only the electrochemical procedure is available for the vast majority of ferrocene derivatives. Moreover, the IR spectroscopic changes associated with oxidation and reduction of such a {M(CO)$_n$}-heteroferrocene biomolecule complex can be investigated in an OTTLE[14] cell. Although such measurements have already proven their value in the case of iron carbonyl [FeFe] hydrogenase models,[9] they have seemingly not been applied to ferrocene and heteroferrocene metal–carbonyl biomarkers.

Despite the above-mentioned advantages offered by M(CO)$_n$–heterometallocene bioconjugates, there is, to the best of our knowledge, only one report in the literature that describes the synthesis of bis-W(CO)$_5$-1,1'-diphosphaferrocene carboxylic acid derivatives[12a] of potential use as IR-detectable biomolecule markers. However, even in that report the question of their electrochemical and IR spectroelectrochemical properties was not addressed. As part of our ongoing program on azaferrocene chemistry, we turned our attention to the biological[12d,12e] and electrochemical[15] properties of selected 2,5-dimethylazaferrocene-derivatives. In an attempt to obtain azaferrocene-based IR-detectable markers of amino group containing (bio)molecules we report herein the synthesis, structure, electrochemistry, and FTIR spectroelectrochemistry of W(CO)$_5$ complexes of 4-oxo-4-(2,5-dimethylazaferrocen-1'-yl)butanoic and 5-oxo-5-(2,5-dimethylazaferrocen-1'-yl)pentanoic acids. The former complex was transformed into its active ester and treated with glycine methyl ester to give the corresponding amide in almost quantitative yield. In contrast to the majority of ferrocene-based tracers utilized so far in biomolecule labeling, our complexes offer dual electrochemical and FTIR channels for their detection. We assume that the electrochemical switching of {M(CO)$_n$}–metallocene macromolecule conjugates combined with their IR spectroscopic analysis will provide useful data sets regarding the local structure and dynamics of the macromolecules. Reported herein are W(CO)$_5$–azaferrocene markers as prototypical, low-cost molecules suitable for checking the basic principles of our idea.

Results and Discussion

Synthesis and Characterization

It has been reported that W(CO)$_5$ complexes of azaferrocenes undergo Friedel–Crafts acylation reactions yielding products with -COR (R = CH$_3$ or CH$_2$CH$_3$) groups solely attached to the Cp ring.[16] In the work described here we have utilized the Friedel–Crafts acylation reaction to obtain target complexes 2 and 3. The procedure involves reaction of the W(CO)$_5$ adduct of 2,5-dimethylazaferrocene (1) with succinic or glutaric anhydride, respectively, in the presence of AlCl$_3$ at room temperature (Scheme 1). In both cases, orange, crystalline, and air-stable products were easily separated from trace amounts of unreacted 1 by column chromatography. Compounds 2 and 3 were characterized by standard spectroscopic methods including ^{1}H NMR, ^{13}C NMR, and IR spectroscopy, MS, and elemental analysis. All analytical data confirm the proposed structures. In addition, complexes 1, 2, and 3 were characterized by cyclic voltammetry and FTIR spectroelectrochemistry. The solid-state structures of 2 and 3 were determined by single-crystal X-ray crystallography (vide infra).
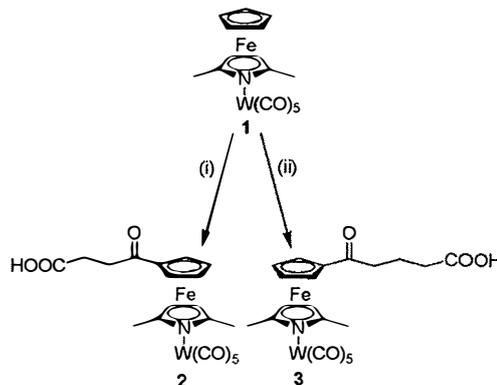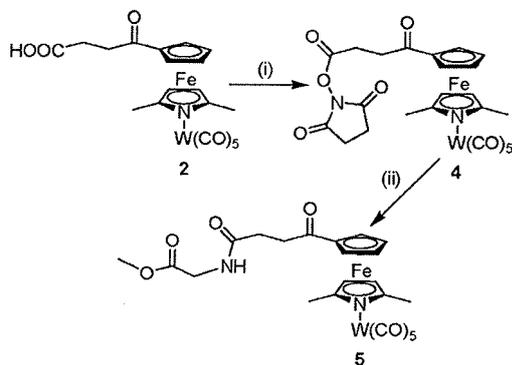

Scheme 1. Synthesis of complexes 2 and 3. Reagents and conditions: (i) AlCl$_3$, succinic anhydride, CH$_2$Cl$_2$, room temp., 30 min; (ii) AlCl$_3$, glutaric anhydride, CH$_2$Cl$_2$, room temp., 30 min.

The ^{1}H NMR spectrum of 2 shows two pseudotriplets at δ = 4.89 and 4.66 ppm for the protons of the substituted cyclopentadienyl ligand and a singlet at δ = 4.74 ppm for the β-pyrrolyl protons. The ^{1}H NMR signals of the CH$_2$CH$_2$ group resonate at δ = 3.05–3.02 and 2.79–2.76 ppm and a singlet of the six α-pyrrolyl methyl protons appears at δ = 2.58 ppm. The most important, structure-confirming ^{13}C NMR signals of 2 are the low-field signals of the CO ligands *trans* and *cis* to the N donor atom at δ = 200.5 and 198.6 ppm, respectively, along with the signals for the carboxylic carbon atom at δ = 177.1 ppm and of the keto carbon atom at δ = 200.4 ppm. The ^{13}C NMR signals of the CH$_2$CH$_2$ group are at δ = 34.4 and 26.8 ppm. The IR spectrum of 2 in 1,2-dichloroethane shows the CO band

pattern characteristic of a C_{4v} arrangement of a M(CO)$_5$ unit with strong bands at 2067, 1923, and 1890 cm^{-1} and a formally forbidden weak band at 1971 cm^{-1}. Identical CO band patterns have been reported for {W(CO)$_5$}-4,4′-bipyridyl, {W(CO)$_5$}pyrazine, and {W(CO)$_5$}ferrocenylpyridine complexes.[17] In chloroform solution the band at 1890 cm^{-1} overlaps with the intense band at 1925 cm^{-1}. The two C=O stretching bands of the carboxylic and keto functions are located at 1743 and 1681 cm^{-1}, respectively. The ^{1}H NMR spectrum of 3 shows two pseudotriplets at δ = 4.83 and 4.65 ppm for the protons of the substituted cyclopentadienyl ligand, a singlet at δ = 4.62 ppm for the β-pyrrolyl protons, two triplets at δ = 2.83 and 2.52 ppm for the outer propylene CH$_2$ groups, a singlet at δ = 2.56 ppm for the two α-pyrrolyl methyl groups, and a multiplet at δ = 2.08–2.01 ppm for the internal CH$_2$ group. The most significant ^{13}C NMR resonances of 3 are the low-field signals of the CO ligands at δ = 202.0 and 198.5 ppm along with the signal of the carboxylic carbon atom at δ = 177.7 ppm and the carbon atom of the keto group at δ = 200.4 ppm. The ^{13}C NMR signals of the propylene group appear at δ = 38.9, 32.5, and 18.7 ppm. The IR spectrum of 3 in chloroform shows three metal–carbonyl bands in the metal–CO region at 2067, 1971, and 1925 cm^{-1} and two C=O stretching bands of the carboxylic and keto functions at 1722 and 1678 cm^{-1}, respectively.

Complex 2 was then transformed into the corresponding N-succinimidyl ester 4 by a standard reaction with N-hydroxysuccinimide (NHS) and N,N′-diisopropylcarbodiimide (DIC) in dichloromethane (Scheme 2). N-Succinimidyl ester 4 was characterized by ^{1}H NMR and IR spectroscopy, MS, and elemental analysis. Once being obtained and characterized, the reactivity of ester 4 toward amino acid derivatives was tested in the reaction with glycine methyl ester (Scheme 2).

Scheme 2. Synthesis of complexes 4 and 5. Reagents and conditions: (i) N-hydroxysuccinimide, N,N′-diisopropylcarbodiimide, CH$_2$Cl$_2$, room temp., 40 min; (ii) glycine methyl ester hydrochloride, triethylamine, CH$_2$Cl$_2$, room temp., overnight.

The readily available glycine ester was chosen as a mimic of the NH$_2$ terminus of peptide chains. The reaction itself was conducted at room temperature in dichloromethane in the presence of triethylamine and gave amino acid bioconjugate 5 in 82% yield. The use of dichloromethane instead

of water as a solvent differs from common reaction conditions for protein labeling.[1] We believe, however, that this disadvantage could be overcome by the application of water–organic solvent mixtures instead of pure water in the course of protein labeling with 4. Compound 5 was characterized by ^{1}H NMR, ^{13}C NMR, and IR spectroscopy, MS, and elemental analysis. All analytical data confirm the proposed structures. Bioconjugate 5 was additionally characterized by cyclic voltammetry and FTIR spectroelectrochemical measurements.

The ^{1}H NMR spectrum of 5 shows a singlet at δ = 6.24 ppm for the amide proton, two pseudotriplets at δ = 4.87 and 4.63 ppm for the protons of the substituted cyclopentadienyl ligand, a singlet at δ = 4.81 ppm for the β-pyrrolyl protons, a doublet at δ = 4.07 ppm for the glycine CH$_2$ group, a singlet at δ = 3.77 ppm for the CH$_3$O group, two triplets at δ = 3.09 and 2.64 ppm for the CH$_2$CH$_2$ group, and a singlet at δ = 2.57 ppm for the two α-pyrrolyl methyl groups. The most diagnostic signals in the ^{13}C NMR spectrum of 5 are the {W(CO)$_5$} resonances of the CO ligands at δ = 201.3 (trans) and 198.6 ppm (cis), along with the signals for the keto carbon atom at δ = 200.5 ppm, the amide carbon atom at δ = 171.9 ppm, and the ester carbon atom at δ = 170.2 ppm. The carbon atoms of the CH$_2$CH$_2$ group resonate at δ = 34.7 and 28.8 ppm, whereas the glycine CH$_2$ carbon atom signal appears at δ = 41.3 ppm. The IR spectrum of 5 in 1,2-dichloroethane shows metal–carbonyl bands at 2067, 1971, 1923, and 1890 cm^{-1} and two C=O stretching bands of the carboxylic and keto functions at 1743 and 1681 cm^{-1}, along with characteristic amide band at 1520 cm^{-1}.

X-ray Crystal Structures

The molecular structures of 2 and 3 were determined by single-crystal X-ray diffraction techniques. Data pertaining to the data collection and structure refinement are given in Table 3. Table S1 provides a selection of the most important interatomic distances and torsion angles. Complexes 2 and 3 differ by just one CH$_2$ group and thus only the representative structure of 3 is displayed in Figure 1 and will be briefly discussed here. We note that the unit cell of crystalline 2 (Figure S1) contains a pair of slightly different conformers 2a and 2b. They are involved, along with one molecule of water, in the formation of several H-bonding interactions, which are graphically presented and discussed in the Supporting Information (Figure S2 and Table S2).

Complex 3 crystallizes with one independent molecule in a general position in the crystallographic unit cell. The pyrrolyl and cyclopentadienyl ligand planes in 3 are inclined towards each other by 2.4°. The iron atom is symmetrically displaced between the different cyclic π perimeters with distances of 1.654(2) Å to the centroid of the substituted cyclopentadienyl ring and of 1.653(2) Å to the pyrrolyl ring. The azaferrocene unit in 3 adopts a conformation intermediate between staggered and eclipsed with a φ angle of 19.6(7)°. The hydrocarbyl chain is located in a plane nearly parallel
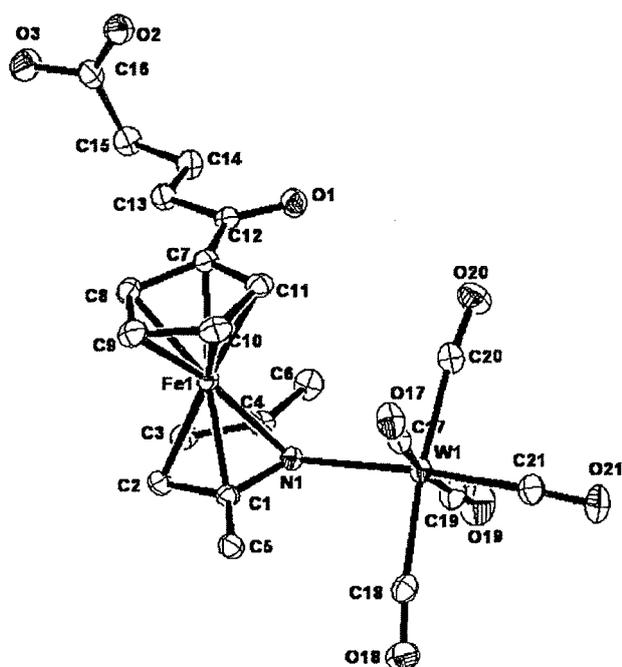
Figure 1. ORTEP plot of the molecular structure of complex **3**. Ellipsoids are drawn at the 50% probability level. Selected bond lengths [Å] and angles [°]: Fe1–Pyr$_{centr}$ 1.653(2), Fe1–Cp$_{centr}$ 1.654(2), N1–C4 1.407(2), N1–C1 1.410(2), O1–C12 1.224(2), O2–C16 1.227(2), O3–C16 1.315(2), W1–N1 2.2875(14), W1–C21 1.9661(19), W1–C20 2.039(2); C11–C7–C12–O1 2.33(17), C12–C13–C14–C15 –175.87(16), C13–C14–C15–C16 71.2(2).

to the Cp plane and is slightly bent away from the azaferrocene sandwich unit. The carboxylic group is rotated to above the plane of the hydrocarbyl chain by 71.2(2)°. The carboxylic groups of individual molecules are related by a crystallographic inversion center and show the hydrogen-bonding pattern characteristic of carboxylic acid dimers as is illustrated in Figure S3. Geometrical details are presented in Table S2. The geometry at the tungsten center is a slightly distorted octahedron. The average value of the *cis* N–W–CO bond angles is 93.3°, whereas the *trans* N–W–CO bond angle is 173.8°. The tungsten center in **3** is displaced out of the plane of the pyrrolyl ring, as is reflected by the Pyr$_{centr}$–N–W angle of 173.9°. The W–CO bond *trans* to the nitrogen atom [1.9661(19) Å] is noticeably shorter than the others [range between 2.35(2) and 2.0453(19) Å].

Electrochemistry

The electrochemical properties of **1**, **2**, **3**, **5** and of the structurally related 1′-acetylazaferrocene **6** (Figure 2) were determined by cyclic voltammetry (CV) in Bu₄NPF₆/CH₂Cl₂ at room temperature. Figures 3 and 4 show voltammograms of **3** and **6**, whereas Figures S4 and S5 show voltammograms of **1** and **5**. Table 1 lists electrochemical data for the complete series of compounds along with electrochemical data of 2,5-dimethylazaferrocene (**7**; Figure 2) as

a comparison. The synthesis and characterization of complex **6** has recently been reported;[16] however, no electrochemical data were given.
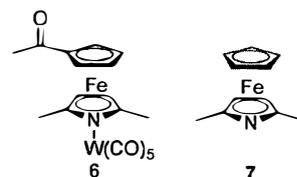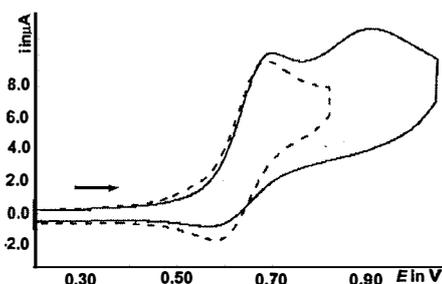

Figure 2. The structures of compounds **6** and **7**.

Figure 3. Cyclic voltammograms of **3** in CH₂Cl₂/NBu₄PF₆ (0.1 M) at ν = 0.3 V s⁻¹ at 295 K.

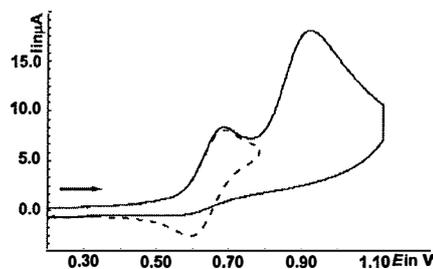
Figure 4. Cyclic voltammograms of **6** in CH₂Cl₂/NBu₄PF₆ (0.1 M) at ν = 0.3 V s⁻¹ at 295 K.

All investigated dinuclear complexes contain one azaferrocene and one W(CO)₅ moiety, both of which are redox active. This is reflected by the presence of two waves in the anodic scans of **1–6**. We assign the wave at the less positive potential as a 2,5-dimethylazaferrocene-based oxidation and the second wave as the oxidation of the W(CO)₅ unit. The potential at which the oxidation of the 2,5-dimethylazaferrocene occurs in **1** is shifted by approximately +0.3 V when compared to 2,5-dimethylazaferrocene.[15b] This large anodic shift of the first oxidation potential clearly indicates that the pyrrolyl ring contributes significantly to the so-called "redox-orbital". In fact, 2,5-dimethylazaferrocene has been described as a good σ-donor and weak π-acceptor toward M(CO)₅ (M = Cr, Mo, W) fragments.[13h] For all compounds, the second wave is irreversible at all scan rates employed. The first wave is chemically reversible for **1** but only partially so for **6**, **2**, and **3** if the potential is switched prior to reaching the second wave but becomes irreversible when the second wave was scanned. The first oxidation of

Table 1. Cyclic voltammetric data for compounds **1, 2, 3, 5, 6**, and **7** obtained at a scan rate of 0.3 V s^{-1} at 295 K in CH$_2$Cl$_2$/Bu$_4$NPF$_6$ (0.1 M) as the supporting electrolyte.

Compound	$E_{1/2}^{0/+}$ [V][a]	ΔE_p [mV][c]	kr[e]	$E_{p,a}(II)^{+/n+}$ [V][f]	$\Delta E_{p,a}$ [mV][g]	$E_{1/2}^{0/+} - E_{p,a}(II)^{+/n+}$ [mV]
1	0.497	84 (91)[d]	1.00	0.876	336	378
2	0.623	104 (88)[d]	0.61	0.896	220	273
3	0.634	126(136)[d]	0.72	0.907	208	273
5	0.673[b]	–	–	0.927	254	–
6	0.640	95 (95)[d]	0.89	0.926	240	286
7	0.174	123(104)[d]	1.00	–	–	–

[a] All potentials are relative to the ferrocene/ferrocenium redox couple, $E_{1/2}^{0/+} = (E_{p,a} + E_{p,c})/2$. [b] Peak potential of an irreversible oxidation process at $v = 0.3$ V s^{-1}. [c] $\Delta E_p = |E_{p,a} - E_{p,c}|$. [d] ΔE_p for ferrocene under the same experimental conditions. [e] $kr = i_{p,rev}/i_{p,forw} + 0.485\ i_r/i_{p,forw} + 0.086$; see ref.[18] [f] Peak potential of an irreversible oxidation process at $v = 0.3$ V s^{-1}. [g] $\Delta E_{p,a} = E_{p,a}(II) - E_{p,a}(I)$.

complex **5**, however, remained irreversible even at high sweep rates. Overall reversibility coefficients defined as the ratio of the total cathodic reverse and the anodic forward currents $i_{p,rev}/i_{p,forw}$ are 1.0 for **1**, 0.61 for **2**, 0.72 for **3**, and 0.89 for **6** at $v = 0.3$ V s^{-1}. Increasing the sweep rates has the effect of increasing the reversibility of the first redox wave but does not affect the reversibility of the second one. Peak-to-peak separations for all azaferrocene-centered oxidation waves are significantly larger than the ideal value of 60 mV for a Nernstian one-electron process. This may be explained by a sum of the uncompensated solution resistance and relatively slow electron-transfer kinetics. Under the same conditions, the ferrocene reference gave ΔE_p values of 88–136 mV. Comparison of the redox potentials of compounds **1** and **2–6** shows that the substitution of a hydrogen atom in **1** by the electron-withdrawing acyl function causes a ca. 140 mV anodic shift of the redox potential of the first wave but has only a minor effect of ca. 40 mV on the potential of the second, irreversible wave.

It is thus apparent that the half-wave potential of the 2,5-dimethylazaferrocene unit in **2–6** is very sensitive to the presence of an electron-accepting substituent. In contrast, the rather constant second oxidation potential indicates only limited interaction between the monooxidized azaferrocene and the W(CO)$_5$ unit. This observation is also reflected by the potential separation between the half-wave potential of the first redox wave and the peak potential of the second, irreversible oxidation, which decreases from ca. 380 mV in **1** to ca. 280 mV in **2–6**. The presence of an additional carboxylic group as in **2, 3**, or an amide function as in **5** does not influence the potential of both waves but seemingly renders the associated radical cations more reactive, thus lowering the chemical reversibility of the first 2,5-dimethylazaferrocene-centered redox wave. The overall electrochemical behavior of complexes **1–6** agrees with data accumulated for ferrocene-bridge–W(CO)$_5$-type compounds,[17b,19] which also exhibit two redox waves with a first reversible ferrocene-centered and a second irreversible tungsten-centered oxidation.

FTIR Spectroelectrochemical Measurements

The influence of the W(CO)$_5$ moiety on the first anodic oxidation potential prompted us to examine the effects of

the azaferrocene-based oxidation on the vibrational spectra. We were particularly interested to see whether the v(CO) band shifts of the attached W(CO)$_5$ moiety can serve as a reporter of the azaferrocene oxidation state in keeping with our idea of utilizing W(CO)$_5$–azaferrocene tags as addressable markers for biomolecules. As a proof of principle we performed IR spectroelectrochemical experiments on the simple complex W(CO)$_5$–2,5-dimethylazaferrocene (**1**), its 1′-acetyl derivative **6**, free tracer **2**, and its amide derivative **5**. Figure 5 shows IR spectroscopic changes upon oxidation of **1**, whereas Figure 6 shows analogous data for acid **2**. Table 2 summarizes data for all investigated complexes, whereas the results of IR spectroelectrochemical measurements of **6** are displayed in Figures S6 and S7. Starting at about 30–40% conversion, additional absorption bands of
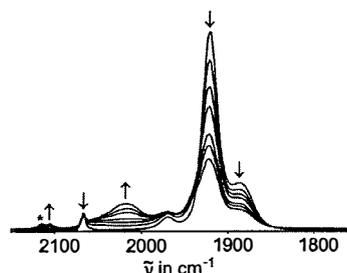

Figure 5. Spectroscopic changes upon (partial) oxidation of complex **1** (NBu$_4$PF$_6$/1,2-C$_2$H$_4$Cl$_2$, room temp.). The star symbol denotes a band of a decomposition product.
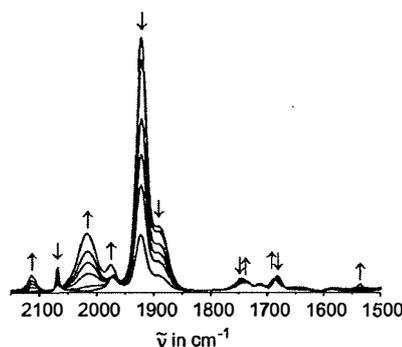

Figure 6. Spectroscopic changes upon (partial) oxidation of complex **2** (NBu$_4$PF$_6$/1,2-C$_2$H$_4$Cl$_2$, room temp.).

Table 2. Spectroscopic data of **1**, **2**, and **6** and their oxidation products as determined by FTIR spectroelectrochemistry.

Compound	ν(CH) [cm⁻¹][b]	ν(W–CO) [cm⁻¹][b]	ν(CO) [cm⁻¹][b]
1	3114 (w)	2066 (m), 1969 (w), 1920 (s), 1886 (s)	–
1·⁺	3119 (w)	2105 (w), 2016 (m), 1970 (s)	–
6	3114 (w), 3109 (w)	2067 (m), 1971 (w), 1923 (s), 1891 (s)	1678 (w)
6·⁺	3124 (w), 3114 (w)	2115 (w), 2020 (m), 1975 (s)	1684 (s)
2	3114 (w), 3099 (w)	2067 (m), 1971 (w), 1923 (s), 1890 (s)	1745 (w), 1681 (m)
2·⁺[a]	3124 (w), 3115 (w)	2115 (w), 2015 (m), 1975 (s)	1742 (w), 1686 (m)

[a] Other bands of **2·⁺** are observed at 3270 and 1535 cm⁻¹. [b] w, weak; s, strong; m, medium.

follow products began to rise with a peak at ca. 2105 cm⁻¹ and a broadening of the feature near 2065 cm⁻¹. Stopping the electrolysis at an oxidation level of ca. 50 to 75% and scanning back past the +/0 peak led to partial recovery of the bands of the parent neutrals at the expense of the bands of the radical cations, supporting our assignment. No useful results could, however, be obtained for **5**. In keeping with the chemical irreversibility of the **5**⁰/⁺ wave observed in voltammetry, rapid decomposition accompanying oxidation did not allow us to accumulate sufficient amounts of the **5**·⁺ radical cation in solution to identify its spectroscopic fingerprint.

Despite these obvious trade-offs, some interesting conclusions can be drawn from these experiments. Most importantly, azaferrocene oxidation induces sizeable blueshifts in the CO bands of the pyrrolyl-bonded W(CO)₅ moiety, whereas there is only a relatively small shift of the keto functionality at the non-heteroatom-substituted cyclopentadienyl ring. This becomes particularly evident when the results on **6** and **2** are compared to those on the acetylferrocene/acetylferrocenium couple. The latter system shows a substantially larger acetyl CO band shift of 34 cm⁻¹ upon oxidation.[20] The shift of the charge-sensitive ν(C–H) stretch of the cyclopentadienyl ring is also considerably smaller than that of 20 cm⁻¹ for ferrocene itself.[21] Along with the large sensitivity of the first oxidation potential to the presence of the W(CO)₅ moiety this provides experimental evidence for the larger contribution of the pyrrolyl ring compared to the cyclopentadienyl ring to the frontier orbitals of azaferrocene–Lewis acid adducts, as it has already been deduced from quantum chemical investigations on the azaferrocene–BH₃ system.[22] Our results unambiguously document that the IR band shifts of the W(CO)₅ moiety are highly sensitive toward the azaferrocene oxidation state. In contrast, the inherently high reactivity of amide radical cation **5**·⁺ indicates that this particular bioconjugate cannot be detected under aqueous or physiological conditions.

Conclusions

We have synthesized the first metal–carbonylazaferrocene-based markers for NH₂ containing (bio)molecules. Their syntheses are simple and the target complexes are air stable. X-ray diffraction analyses have revealed that hydrogen-bonding networks stabilize the crystallographic lattice. One of the complexes was transformed into an active ester

and then treated with glycine methyl ester. The corresponding amide exhibited sharp intense absorption bands in the metal–CO region, which demonstrate the utility of metal–carbonylazaferrocene derivatives as IR-detectable markers. In an attempt to further explore electrochemical and FTIR spectroelectrochemical ways of detection of our compounds, we subjected them toward cyclic voltammetry and FTIR spectroelectrochemical measurements. The cyclic voltammetry study revealed two redox events. The first, azaferrocene-centered process is partially reversible, whereas the second, W(CO)₅-centered process involves more than one electron. FTIR spectroelectrochemical measurements revealed that the oxidized forms of metal–carbonylazaferrocene derivatives possess only limited lifetimes. Despite this disadvantage, our results indicate that the IR band shift of the W(CO)₅ moiety is highly sensitive toward changing the azaferrocene oxidation state. We are now screening reporter groups other than W(CO)₅ in order to improve the stabilities of their oxidized forms for FTIR spectroelectrochemical markers with superior performance.

Experimental Section

General Comments: All preparations were carried out by using standard Schlenk techniques. Chromatographic separations were carried out by using silica gel 60 (Merck, 230–400 mesh ASTM). Dichloromethane (DCM) was distilled from CaH₂ prior to use. Other solvents were of reagent grade and were used without prior purification. All other chemicals were purchased from the Aldrich Chemical Co. The NMR spectra were recorded with Bruker AV400 (400 MHz) and Varian Gemini 200BB (200 MHz) spectrometers. Chemical shifts are reported in δ (ppm) using residual CHCl₃ (¹H δ = 7.26 ppm) as the reference. Mass spectra were recorded using EI methods with a Finnigan MAT 710A spectrometer and ESI methods using a Varian 500MS LC spectrometer. IR spectra were recorded with an FTIR Nexus Nicolet apparatus. Microanalyses were determined by Analytical Services of the Polish Academy of the Sciences (Łódź). 2,5-Dimethylazaferrocene[23] and W(CO)₅–2,5-dimethylazaferrocene[13h] were prepared according to literature procedures.

4-Oxo-4-(2,5-dimethylazaferrocen-1′-yl)butanoic Acid W(CO)₅ Complex 2: W(CO)₅–2,5-dimethylazaferrocene (**1**; 253 mg, 0.46 mmol) dissolved in dichloromethane (13 mL) was treated with succinic anhydride (90 mg, 0.9 mmol) and AlCl₃ (200 mg, 1.5 mmol). The orange coloration of the reaction mixture turned gradually violet. After 30 min at room temperature, the reaction mixture was poured into a saturated aqueous solution of Na₂CO₃. Resulting dichloromethane and water phases were separated. Both were then treated with ca. 20% aqueous HCl, and the water phase was extracted with

Et$_2$O. The ether phase was dried with MgSO$_4$ and combined with the dichloromethane one. The resulting solution was evaporated to dryness. The residue was dissolved in CHCl$_3$/MeOH (50:4) and subjected to column chromatography on SiO$_2$ (CHCl$_3$/MeOH, 50:4). Two fractions were collected: a first, small one, containing 1 (8 mg) and a second one containing 2 (orange solid) in 70% (205 mg) yield. ^{1}H NMR (400 MHz, CDCl$_3$): δ = 4.89 (pseudo-t, $J_{H,H}$ = 1.6 Hz, 2 H, C$_5$H$_4$), 4.74 (s, 2 H, β-pyrrolyl), 4.66 (pseudo-t, $J_{H,H}$ = 1.6 Hz, 2 H, C$_5$H$_4$), 3.05–3.02 (m, 2 H, CH$_2$), 2.79–2.76 (m, 2 H, CH$_2$), 2.58 (s, 6 H, CH$_3$) ppm. ^{13}C NMR (100 MHz, CDCl$_3$): δ = 200.5 (trans-CO), 200.4 (C=O), 198.6 (cis-CO), 177.1 (COOH), 106.8 (α-pyrrolyl), 78.5 (C$_5$H$_4$), 78.1 (ipso-C$_5$H$_4$), 74.1 (β-pyrrolyl), 71.2 (C$_5$H$_4$), 34.4 (CH$_2$), 26.8 (CH$_2$), 18.8 (αCH$_3$-pyrrolyl) ppm. MS (EI, 70 eV): m/z = 592 [M – HCOOH]$^+$, 564 [M – HCOOH – CO]$^+$, 536 [M – HCOOH – 2CO]$^+$, 508 [M – HCOOH – 3CO]$^+$, 480 [M – HCOOH – 4CO]$^+$, 94 [C$_6$H$_8$N]$^+$, 44 [CO$_2$]$^+$. FTIR (CHCl$_3$): $\tilde{v}$ = 2067 (m, v$_{W-CO}$), 1971 (w, v$_{W-CO}$), 1925 (s, v$_{W-CO}$), 1728 (w, v$_{C=O,acid}$), 1682 (m, v$_{C=O,ketone}$) cm^{-1}. FTIR (C$_2$H$_4$Cl$_2$): $\tilde{v}$ = 2067 (m, v$_{W-CO}$), 1971 (w, v$_{W-CO}$), 1923 (s, v$_{W-CO}$), 1890 (s, v$_{W-CO}$), 1743 (w, v$_{C=O,acid}$), 1681 (m, v$_{C=O,ketone}$) cm^{-1}. C$_{20}$H$_{17}$FeNO$_8$W (639.05): calcd. C 37.59, H 2.68, N 2.19; found C 37.29, H 2.69, N 2.27.

5-Oxo-5-(2,5-dimethylazaferrocen-1'-yl)pentanoic Acid W(CO)$_5$ Complex 3:

Synthesis was performed as for 2 but with glutaric anhydride (114 mg, 1.0 mmol). Yield 156 mg (52%). ^{1}H NMR (400 MHz, CDCl$_3$): δ = 4.83 (pseudo-t, $J_{H,H}$ = 1.6 Hz, 2 H, C$_5$H$_4$), 4.65 (pseudo-t, $J_{H,H}$ = 1.6 Hz, 2 H, C$_5$H$_4$), 4.62 (s, 2 H, β-pyrrolyl), 2.83 (t, $J_{H,H}$ = 7.2 Hz, 2 H, CH$_2$), 2.56 (s, 6 H, CH$_3$), 2.52 (t, $J_{H,H}$ = 7.2 Hz, 2 H, CH$_2$), 2.08–2.01 (m, 2 H, CH$_2$) ppm. ^{13}C NMR (100 MHz, CDCl$_3$): δ = 202.0 (trans-CO), 200.4 (C=O), 198.5 (cis-CO), 177.7 (COOH), 106.6 (α-pyrrolyl), 79.3 (ipso-C$_5$H$_4$), 77.9 (C$_5$H$_4$), 73.9 (β-pyrrolyl), 71.4 (C$_5$H$_4$), 38.9 (CH$_2$), 32.5 (CH$_2$), 18.8 (αCH$_3$-pyrrolyl), 18.7 (CH$_2$) ppm. MS (EI, 70 eV): m/z = 592 [M – CH$_3$COOH – H]$^+$, 564 [M – CH$_3$COOH – H – CO]$^+$, 536 [M – CH$_3$COOH – H – 2CO]$^+$, 508 [M – CH$_3$COOH – H – 3CO]$^+$, 480 [M – CH$_3$COOH – H – 4CO]$^+$, 452 [M – CH$_3$COOH – H – 5CO]$^+$, 94 [C$_6$H$_8$N]$^+$. FTIR (CHCl$_3$): $\tilde{v}$ = 2067 (m, v$_{W-CO}$), 1971 (w, v$_{W-CO}$), 1925 (s, v$_{W-CO}$), 1722 (w, v$_{C=O, acid}$), 1678 (w, v$_{C=O,ketone}$) cm^{-1}. FTIR (C$_2$H$_4$Cl$_2$): $\tilde{v}$ = 2067 (m, v$_{W-CO}$), 1971 (w, v$_{W-CO}$), 1923 (s, v$_{W-CO}$), 1890 (s, v$_{W-CO}$), 1743 (w, v$_{C=O,acid}$), 1681 (m, v$_{C=O,ketone}$) cm^{-1}. C$_{21}$H$_{19}$FeNO$_8$W (653.08): calcd. C 38.62, H 2.93, N 2.14; found C 38.84, H 3.05, N 2.19.

N-Succinimidyl Ester 4:

To a solution of 2 (78 mg, 0.12 mmol) in dichloromethane (5 mL) was added N-hydroxysuccinimide (14 mg, 0.12 mmol) and N,N'-diisopropylcarbodiimide (15.14 mg, 0.12 mmol). After 40 min the solvent was evaporated under reduced pressure. The residue was dissolved in CHCl$_3$ and subjected to flash chromatography. Product 3 was obtained as an orange-red solid in 95% (84 mg) yield. ^{1}H NMR (200 MHz, CDCl$_3$): δ = 4.90 (pseudo-t, $J_{H,H}$ = 2.0 Hz, 2 H, C$_5$H$_4$), 4.71 (s, 2 H, β-pyrrolyl), 4.66 (pseudo-t, $J_{H,H}$ = 2.0 Hz, 2 H, C$_5$H$_4$), 3.19–3.09 (m, 2 H, CH$_2$), 3.09–3.00 (m, 2 H, CH$_2$), 2.87 (s, 4 H, succinimide), 2.58 (s, 6 H, CH$_3$) ppm. MS (ESI): m/z = 759 [M + Na]$^+$. FTIR (CHCl$_3$): $\tilde{v}$ = 2067 (m, v$_{W-CO}$), 1971 (w, v$_{W-CO}$), 1925 (s, v$_{W-CO}$), 1817 (w, v$_{C=O,imide}$), 1788 (w, v$_{C=O,imide}$), 1743 (m, v$_{C=O, ester}$), 1682 (w, v$_{C=O,ketone}$) cm^{-1}. C$_{24}$H$_{20}$N$_2$O$_{10}$FeW+CH$_3$OH (768.17): calcd. C 39.09, H 3.15, N 3.65; found C 38.89, H 3.35, N 4.12.

Synthesis of Bioconjugate 5:

Active ester 4 (84 mg, 0.11 mmol) was dissolved in dichloromethane (3 mL). To this solution was added a solution of glycine methyl ester hydrochloride (16 mg, 0.13 mmol) in dichloromethane (2 mL) containing triethylamine (4 drops), and the resulting solution was stirred overnight at room temperature.

The solvent was evaporated to dryness, and the residue was subjected to column chromatography on SiO$_2$ (CHCl$_3$/MeOH, 50:4). Product 5 was obtained as an orange oily solid in 82% (64 mg) yield. ^{1}H NMR (400 MHz, CDCl$_3$): δ = 6.24 (s, 1 H, N-H), 4.87 (pseudo-t, $J_{H,H}$ = 1.6 Hz, 2 H, C$_5$H$_4$), 4.81 (s, 2 H, β-pyrrolyl), 4.63 (pseudo-t, $J_{H,H}$ = 1.6 Hz, 2 H, C$_5$H$_4$), 4.07 (d, $J_{H,H}$ = 5.2 Hz, 2 H, CH$_2$), 3.77 (s, 3 H, OCH$_3$), 3.09 (t, $J_{H,H}$ = 6 Hz, 2 H, CH$_2$), 2.64 (t, $J_{H,H}$ = 6 Hz, 2 H, CH$_2$), 2.57 (s, 6 H, CH$_3$) ppm. ^{13}C NMR (100 MHz, CDCl$_3$): δ = 201.3 (trans-CO), 200.5 (C=O), 198.6 (cis-CO), 171.9 (CONH), 170.2 (COOCH$_3$), 106.8 (α-pyrrolyl), 78.5 (C$_5$H$_4$), 78.1 (ipso-C$_5$H$_4$), 74.3 (β-pyrrolyl), 71.1 (C$_5$H$_4$), 52.3 (OCH$_3$), 41.3 (NH-CH$_2$-COOCH$_3$), 34.7 (CH$_2$), 28.8 (CH$_2$), 18.8 (αCH$_3$-pyrrolyl) ppm. MS (ESI): m/z = 710 [M]$^+$. FTIR (CHCl$_3$): $\tilde{v}$ = 2067 (m, v$_{W-CO}$), 1971 (w, v$_{W-CO}$), 1925 (s, v$_{W-CO}$), 1747 (m, v$_{C=O,ester}$), 1680 (m, v$_{C=O,ketone}$), 1520 (m, v$_{amide\ bending}$) cm^{-1}. FTIR (C$_2$H$_4$Cl$_2$): $\tilde{v}$ = 2067 (m, v$_{W-CO}$), 1971 (w, v$_{W-CO}$), 1923 (s, v$_{W-CO}$), 1890 (s, v$_{W-CO}$), 1743 (w, v$_{C=O,ester}$), 1681 (m, v$_{C=O,ketone}$) cm^{-1}. C$_{23}$H$_{22}$FeN$_2$O$_9$W (710.11): calcd. C 38.90, H 3.12, N 3.94; found C 38.98, H 3.12, N 4.07.

X-ray Crystallography:

Crystals suitable for X-ray analysis were obtained by slow diffusion of n-hexane into a concentrated solution of the complex in chloroform. The data for 2 and 3 were collected by using a Bruker Kappa APEXII Ultra controlled by APEXII software,[24] equipped with Mo-K_α rotating anode X-ray source (λ = 0.71073 A, 50.0 kV, 22.0 mA) monochromated by multilayer optics and APEX-II CCD detector. The experiments were carried out at 100 K using an Oxford Cryostream cooling device. The crystals were mounted on thin cactus needle with a droplet of Pantone-N oil and immediately cooled. Indexing, integration, and initial scaling were performed with SAINT and SADABS software.[25] The data collection and processing statistics are reported in tables for according structures. The structures were solved by direct methods approach using the SHELXS-97 program and refined with SHELXL-97.[26] The analytical numeric absorption correction using a multifaceted crystal model was applied in the scaling procedure. The refinement was based on F^2 for all reflections except those with negative intensities. Weighted R factors wR and all goodness-of-fit S values were based on F^2, whereas conventional R factors were based on the amplitudes, with F set to zero for negative F^2. The $F_o^2 > 2\sigma(F_o^2)$ criterion was applied only for R factor calculation was not relevant to the choice of reflections for the refinement. The R factors based on F^2 are for all structures about twice as large as those based on F. The hydrogen atoms were located in idealized geometrical positions. Scattering factors were taken from Tables 4.2.6.8 and 6.1.1.4 from the International Crystallographic Tables Volume C.[27] Details of the data collection and refinement are presented in Table 3. Most of the statistics, and especially Flack parameter of value 0.505(8) for the structure of 2 indicated that centrosymmetric P2$_1$/c could be better applied to describe the crystal structure of the compound. This may be the result of the heavy atom, in particular tungsten, dominating the starting signal. However, closer inspection of the structure, and particularly the analysis of hydrogen-bond network and small but significant differences in the conformations of hydrocarbon chains indicates that the molecules of 2 potentially related by additional inversion center differ significantly enough to be treated as independent molecules. There are high residual density peaks in close vicinity of the tungsten atom in 2 and 3. They are located in a distance of 0.84 Å (highest peak) from the W2 atom and 1.38 Å (deepest hole) from the W2 atom in case of 2. In case of 3 the highest peak is located in a distance of 0.65 Å from the W1 atom and the deepest whole of 1.08 Å from the W1 atom. The peaks may be attributed to aspherical electron density of d orbitals, which can be observed

Table 3. Summary of data collection and refinement statistics for compounds **2** and **3**.

	2	**3**
Formula	$C_{40}H_{36}Fe_2N_2O_{17}W_2$	$C_{21}H_{19}FeNO_8W$
Formula weight	1296.11	653.07
Temperature [K]	100(2)	100(2)
Wavelength [Å]	0.71073	0.71073
Crystal system	monoclinic	triclinic
Space group	Pc	$P\bar{1}$
a [Å]	17.2638(5)	7.2659(2)
b [Å]	9.2320(3)	9.5226(3)
c [Å]	13.4837(5)	16.5668(5)
α [°]	90	102.339(2)
β [°]	106.330(2)	97.600(2)
γ [°]	90	96.6870(10)
Volume [Å^3]	2062.33(12)	1097.48(6)
Z	2	2
$D_{calcd.}$ [g cm^{-3}]	2.087	1.976
Abs. coefficient [mm^{-1}]	6.328	5.945
$F(000)$	1252	632
Crystal size [mm]	$0.28 \times 0.22 \times 0.12$	$0.268 \times 0.213 \times 0.131$
θ range for data collection [°]	1.23–28.46	1.28–32.57
Index ranges	$-21 \leq h \leq 23$	$-11 \leq h \leq 10$
	$-12 \leq k \leq 8$	$-14 \leq k \leq 14$
	$-14 \leq l \leq 18$	$-25 \leq l \leq 25$
Refl. collected/unique	12722/6702	32293/7977
R_{int}	0.0188	0.0244
Absorption correction	semiempirical from equivalents	numerical
Max. and min. transmission	0.477 and 0.210	0.4590 and 0.2320
Refinement method	full-matrix least-squares on F^2	full-matrix least-squares on F^2
Data/restraints/parameters	6702/15/583	7977/0/292
GOF on F^2	1.130	1.070
Final R indices [$I > 2\sigma(I)$]	$R_1 = 0.0193$, $wR_2 = 0.0476$	$R_1 = 0.0187$, $wR_2 = 0.0462$
R indices (all data)	$R_1 = 0.0205$, $wR_2 = 0.0561$	$R_1 = 0.0210$, $wR_2 = 0.0470$
Largest diff. peak and hole [e/Å^3]	1.491 and –0.565	2.089 and –0.484

due to high resolution of diffraction data. Plots of **2** and **3** have been taken from ORTEP-3 for Windows.[28] CCDC-726623 (for **2**) and -726624 (for **3**) contain the supplementary crystallographic data for this paper. These data can be obtained free of charge from The Cambridge Crystallographic Data Centre via www.ccdc.cam. ac.uk/data_request/cif.

Electrochemistry: Electrochemical work was performed with a Princeton Applied Research VersaStat3 potentiostat in a home-built vacuum-tight one-compartment cell using Pt electrodes as the working electrode, a platinum spiral as the counter electrode, and a silver spiral as a pseudo-reference electrode. Each of the spiral-shaped electrodes was welded to a Vycon wire and sealed into a glass tube. Counter and reference electrodes were introduced into the cell by appropriate fittings in the side-wall and sealed by a Quickfit screw. CH_2Cl_2 for electrochemical use was of Burdick & Jackson brand (Fluka) and was distilled from CaH_2, deoxygenated by saturation with argon, and briefly stored over molecular sieves. Potential calibration was performed by adding ferrocene as an internal standard to the analyte solution. The amount of the reference system was adjusted until its peak currents were comparable to those of the analyte. Potentials are given against the ferrocene/ ferrocenium couple.

Supporting Information (see footnote on the first page of this article): Bonds lengths and angles of **2a**, **2b**, and **3**; ORTEP plot of the structures of the two conformers of **2** along a figure showing the graphical representation of the network of intermolecular hydrogen bonds present within the crystal of **2**; hydrogen-bond pattern in dimers of **3**; detailed description of the hydrogen-bonding interac-

tions present in **2** and **3**; IR spectroscopic changes during the oxidation/reduction of **6/6**$^{·+}$; CV of **1** and **5**.

[1] G. Jaouen (Ed.), *Bioorganometallics: Biomolecules, Labeling, Medicine*, Wiley-VCH, New York, **2006**, and references cited therein.
[2] a) D. Schlawe, A. Majdalani, J. Velcicky, E. Heßler, T. Wieder, A. Prokop, H.-G. Schmalz, *Angew. Chem. Int. Ed.* **2004**, *43*, 1731–1734; b) P. James, J. Neudörfl, M. Eissmann, P. Jesse, A. Prokop, H.-G. Schmalz, *Org. Lett.* **2006**, *8*, 2763–2766.
[3] C. D. Sergeant, I. Ott, A. Sniady, S. Meneni, R. Gust, A. L. Rheingold, R. Dembinski, *Org. Biomol. Chem.* **2008**, *6*, 73–80.

[4] a) K. Schmidt, M. Jung, R. Keilitz, B. Schnurr, R. Gust, *Inorg. Chim. Acta* **2000**, *306*, 6–16; b) I. Ott, K. Schmidt, B. Kircher, P. Schumacher, T. Wiglenda, R. Gust, *J. Med. Chem.* **2005**, *48*, 622–629; c) I. Ott, B. Kircher, C. P. Bagowski, D. H. W. Vlecken, E. B. Ott, J. Will, K. Bensdorf, W. S. Sheldrick, R. Gust, *Angew. Chem. Int. Ed.* **2009**, *48*, 1160–1163.

[5] a) H. Bergman, D. S. Williams, G. E. Atilla, P. J. Carroll, E. Meggers, *J. Am. Chem. Soc.* **2004**, *126*, 13594–13595; b) D. S. Williams, G. E. Atilla, H. Bregman, A. Arzoumaniam, P. S. Klein, E. Meggers, *Angew. Chem. Int. Ed.* **2005**, *44*, 1984–1987; c) G. E. Atilla-Gokcumen, N. Pagano, C. Streu, J. Maksimoska, P. Filippakopoulos, S. Knapp, E. Meggers, *ChemBioChem* **2008**, *9*, 2933–2936.

[6] a) M. A. Neukamm, A. Pinto, N. Metzler-Nolte, *Chem. Commun.* **2008**, 232–234; b) G. Gasser, M. A. Neukamm, A. Ewers, O. Brosch, T. Weyhermüller, N. Metzler-Nolte, *Inorg. Chem.* **2009**, *48*, 3157–3166.

[7] a) T. R. Johnson, B. E. Mann, J. E. Clark, R. Foresti, C. J. Green, R. Motterlini, *Angew. Chem. Int. Ed.* **2003**, *42*, 3722–3729; b) B. E. Mann, R. Motterlini, *Chem. Commun.* **2007**, 4197–4208; c) J. Niesel, A. Pinto, H. W. Peindy N'Dongo, K. Merz, I. Ott, R. Gust, U. Schatzschneider, *Chem. Commun.* **2008**, 1798–1800.

[8] a) H. W. Peindy N'Dongo, I. Ott, R. Gust, U. Schatzschneider, *J. Organomet. Chem.* **2009**, *694*, 823–827.

[9] a) T. Liu, M. Darensbourg, *J. Am. Chem. Soc.* **2007**, *129*, 7008–7009; b) J.-F. Capon, F. Gloaguen, F. Y. Pétillon, P. Schollhammer, J. Talarmin, *Eur. J. Inorg. Chem.* **2008**, 4671–4681; c) A. K. Justice, M. J. Nilges, T. B. Rauchfuss, S. R. Wilson, L. De Gioia, G. Zampella, *J. Am. Chem. Soc.* **2008**, *130*, 5293–5301; d) Ch. M. Thomas, T. Liu, M. Hall, B. Hall, M. Y. Darensbourg, *Inorg. Chem.* **2008**, *47*, 7009–7024; e) A. K. Justice, L. De Gioia, M. J. Nilges, T. B. Rauchfuss, S. R. Wilson, G. Zampella, *Inorg. Chem.* **2008**, *47*, 7405–7414; f) X. de Hatten, E. Bothe, K. Merz, I. Huc, N. Metzler-Nolte, *Eur. J. Inorg. Chem.* **2008**, 4530–4537.

[10] a) D. R. van Staveren, N. Metzler-Nolte, *Chem. Rev.* **2004**, *104*, 5931–5986; b) N. Metzler-Nolte, M. Salmain in *Ferrocenes: Ligands, Materials and Biomolecules* (Ed.: P. Štěpnička), Wiley-VCH, Chichester, **2008**, ch. 13.

[11] a) S. Top, J. Tang, A. Vessières, D. Carrez, C. Provot, G. Jaouen, *Chem. Commun.* **1996**, 955–956; b) S. Top, B. Dauer, J. Vaissermann, G. Jaouen, *J. Organomet. Chem.* **1997**, *541*, 355–361; c) S. Top, A. Vessières, C. Cabestaing, I. Laios, G. Leclercq, C. Provot, G. Jaouen, *J. Organomet. Chem.* **2001**, *637*, 500–506; d) S. Top, A. Vessières, G. Leclercq, J. Quivy, J. Tang, J. Vaissermann, M. Huché, G. Jaouen, *Chem. Eur. J.* **2003**, *9*, 5223–5236; e) E. Hillard, A. Vessières, L. Thouin, G. Jaouen, Ch. Amatore, *Angew. Chem. Int. Ed.* **2006**, *45*, 285–290; f) A. Vessières, S. Top, W. Beck, E. Hillard, G. Jaouen, *Dalton Trans.* **2006**, 529–541; g) E. A. Hillard, P. Pigeon, A. Vessières, Ch. Amatore, G. Jaouen, *Dalton Trans.* **2007**, 5073–5081.

[12] a) J. Zakrzewski, A. Kłys, M. Bukowska-Strzyżewska, A. Tosik, *Organometallics* **1998**, *17*, 5880–5886; b) K. Kowalski, A. Vessières, S. Top, G. Jaouen, J. Zakrzewski, *Tetrahedron Lett.* **2003**, *44*, 2749–2751; c) E. A. Hillard, A. Vessières, S. Top, P.

Pigeon, K. Kowalski, M. Huché, G. Jaouen, *J. Organomet. Chem.* **2007**, *692*, 1315–1326; d) K. Kowalski, J. Zakrzewski, N. J. Long, N. Suwaki, D. J. Mann, A. J. P. White, *Dalton Trans.* **2006**, 571–576; e) K. Kowalski, N. Suwaki, J. Zakrzewski, A. J. P. White, N. J· Long, D. J. Mann, *Dalton Trans.* **2007**, 743–748.

[13] a) Ch. Ganter, L. Brassat, C. Glinsböckel, B. Ganter, *Organometallics* **1997**, *16*, 2862–2867; b) C. Kaulen, C. Pala, Ch. Hu, Ch. Ganter, *Organometallics* **2001**, *20*, 1614–1619; c) L. Brassat, B. Ganter, Ch. Ganter, *Chem. Eur. J.* **1998**, *4*, 2148–2153; d) G. E. Herberich, B. Ganter, *Inorg. Chem. Commun.* **2001**, *4*, 100–103; e) X. Sava, N. Mézailles, L. Ricard, F. Mathey, P. Le Floch, *Organometallics* **1999**, *18*, 807–810; f) X. Sava, L. Ricard, F. Mathey, P. Le Floch, *Organometallics* **2000**, *19*, 4899–4903; g) A. Kłys, A. Rybarczyk-Pirek, J. Zakrzewski, *J. Organomet. Chem.* **2008**, *693*, 1166–1170; h) J. Silver, J. Zakrzewski, A. Tosik, M. Bukowska-Strzyżewska, *J. Organomet. Chem.* **1997**, *540*, 169–174; i) K. Kowalski, J. Zakrzewski, L. Jerzykiewicz, *J. Organomet. Chem.* **2005**, *690*, 764–772; j) L. Jerzykiewicz, K. Kowalski, J. Zakrzewski, *Acta Crystallogr., Sect. E* **2006**, *62*, 1832–1834; k) K. Kowalski, A. J. P. White, *Acta Crystallogr., Sect. E* **2007**, *63*, 392–393.

[14] M. Krejčik, M. Daněk, F. Hartl, *J. Electroanal. Chem.* **1991**, *317*, 179–187.

[15] a) K. Kowalski, J. Zakrzewski, M. Palusiak, S. Domagała, *New J. Chem.* **2006**, *30*, 901–907; b) K. Kowalski, R. F. Winter, *J. Organomet. Chem.* **2008**, *693*, 2181–2187; c) K. Kowalski, R. F. Winter, *J. Organomet. Chem.* **2009**, *694*, 1041–1048.

[16] K. Kowalski, J. Zakrzewski, L. Jerzykiewicz, *J. Organomet. Chem.* **2005**, *690*, 1474–1477.

[17] a) M. W. George, F. P. A. Johnson, J. J. Turner, J· R. Westwell, *J. Chem. Soc., Dalton Trans.* **1995**, 2711–2718; b) S. Sakanishi, D. A. Bardwell, S. Couchman, J. C. Jeffery, J. McCleverty, M. D. Ward, *J. Organomet. Chem.* **1997**, *528*, 35–45.

[18] R. S. Nicholson, *Anal. Chem.* **1966**, *38*, 1406–1406.

[19] a) P. Štěpnička, I. Cisařová, *Inorg. Chem.* **2006**, *45*, 8785–8798; b) A. C. Ohs, A. L. Rheingold, M. J. Shaw, Ch. Nataro, *Organometallics* **2004**, *23*, 4655–4660.

[20] M. J. Shaw, W. E. Geiger, *Organometallics* **1996**, *15*, 13–15.

[21] H. P. Fritz, *Adv. Organomet. Chem.* **1964**, *1*, 239–315.

[22] G. Frison, F. Mathey, A. Sevin, *J. Phys. Chem. A* **2002**, *106*, 5653–5659.

[23] J. Zakrzewski, *Inorg. Chim. Acta* **1998**, *278*, 101–102.

[24] a) *APEXII-2008v1.0*, Bruker Nonius, **2007**; b) *SAINT V7.34A*, Bruker Nonius, **2007**.

[25] SADABS-2004/1, Bruker Nonius Area Detector Scaling and Absorption Correction, **2007**.

[26] G. M. Sheldrick, *Acta Crystallogr., Sect. A* **2008**, *64*, 112–122.

[27] a) A. J. C. Wilson (Ed.), *International Tables for Crystallography*, Kluwer, Dordrecht, **1992**, vol. C. WingGX; b) L. J. Farrugia, *J. Appl. Crystallogr.* **1999**, *32*, 837–838.

[28] *ORTEP-3 for Windows*: L. J. Farrugia, *J. Appl. Crystallogr.* **1997**, *30*, 565–565.